applied sciences

MDPI

Article

Calculations of Cross-Sections for Positron Scattering on Benzene

Małgorzata Franz [1,*], Anna Pastuszko [1] and Jan Franz [1,2,*]

[1] Faculty of Applied Physics and Mathematics, Gdańsk University of Technology, 80-233 Gdańsk, Poland
[2] Advanced Materials Center, Gdańsk University of Technology, 80-233 Gdańsk, Poland
* Correspondence: malobaro@pg.edu.pl (M.F.); janfranz@pg.edu.pl (J.F.)

Abstract: In this work, we present a theoretical study on positron scattering by benzene molecules over a broad energy range (1–1000 eV). The aim of this work is to provide missing data from partial cross-sections for specific processes. In particular, calculations of cross-sections for direct ionization and electronic excitation were carried out for benzene molecules in the gas phase. An estimate for the cross-section for positronium formation is obtained from a comparison with the total cross-section from experiments. Theoretical methodologies used in the study for partial ionization cross-section calculations are based on the binary-encounter Bethe model and take into account an extension of the Wannier theory. The total cross-section shows good agreement with experimental data.

Keywords: positron–molecule scattering; positron impact ionization; binary-encounter Bethe; benzene

1. Introduction

Positron interactions with organic molecules play a vital role in medical physics, materials science, and astrophysics [1–7]. In medical physics, particular interest is focused on the positronium (Ps) and its role in positron emission tomography (PET) [1]. Ps atoms, which are short-lived bound states of an electron and its antiparticle, the positron, can be created when a positron is emitted inside the human body and does not annihilate directly with one of the electrons of the examined organism. As research shows, about 40% of the positrons in PET scans decay through Ps formation rather than direct annihilation [1]. Hence, the Ps is being explored as a crucial component of new-generation PET devices. In materials science, positron annihilation spectroscopy methods yield information about defects localizing positrons and can provide identification of neutral or negatively charged vacancy-related defects in materials [2]. It is also possible to identify specific point defects by comparing the experimentally determined lifetimes with Density Functional Theory (DFT)-calculated values for the perfect material state and states localized at specific vacancy-related defects [3]. Furthermore, positron lifetime measurements, which are performed using high-intensity positron beams, enable the determination of a depth profile of vacancy-related defects [3]. Positrons in space are created mainly in the interstellar medium (ISM), when photons or high-energy particles from cosmic radiation trigger a cascade of processes, and positrons are one of the final products [4]. Other sources of these particles are massive stars, as well as red giants and Wolf–Rayet stars [5]. Potential sources also include pulsars, neutron stars, and black holes, as well as dark matter [6]. The spectrum of the photons, created due to positron annihilation in our galaxy, has been examined over a wide range of energies, from 50 keV to over 100 GeV [7]. In the low-energy region (from 50 keV to

check for updates

Academic Editor: Wilhelm Becker

Received: 17 November 2024
Revised: 14 December 2024
Accepted: 26 December 2024
Published: 27 December 2024

Citation: Franz, M.; Pastuszko, A.; Franz, J. Calculations of Cross-Sections for Positron Scattering on Benzene. *Appl. Sci.* **2025**, *15*, 153. https://doi.org/10.3390/app15010153

10 MeV), photon emissions can be explained with good accuracy [8], while in the high-energy region, from 1.5 to 100 GeV, the results of observations suggest an excess of ultra-relativistic positrons in cosmic rays in relation to theoretical models [9,10]. Furthermore, a yet-unresolved problem is to find an explanation for the annihilation radiation map in the ISM. The known astronomical objects in the ISM do not possess the capability to produce such a high rate of positrons that could stay in agreement with the photon emission resulting from their annihilation [9]. A possible explanation could be positron scattering on polycyclic aromatic hydrocarbon (PAH) molecules, which were found in the composition of the interstellar dust [10]. Experimental results of positron–PAH molecule annihilation cross-sections, which show that these increase by several orders of magnitude, seem to confirm the possible importance of such reactions in the ISM [11].

For the theoretical study of positron interaction with matter, knowledge of scattering cross-sections is crucial. In particular, positron-transport Monte Carlo simulation studies, e.g., [12,13], need a set of input data describing the interaction of the positron beam with the target. The cross-sections describe different physical phenomena that occur during the interaction of positrons with the target atoms or molecules. Elastic and inelastic processes particularly need to be considered. For low-energy positron interactions with atoms and molecules, the processes of interest include elastic scattering, electronic and vibrational excitation, ionization, Ps formation, and annihilation [13]. There have been a number of earlier review articles involving cross-sections for positron scattering, e.g., [14]; however, the benzene molecule, which is the simplest aromatic hydrocarbon, has not received considerable attention in positron scattering studies.

The motivation for this paper is to provide cross-section data for positron–benzene scattering, particularly for cross-sections of direct ionization, which are interesting for applications, e.g., in the further development of PET technology [1,13]. New-generation PET scanners utilize Ps as a biomarker [15,16]. For a deeper understanding of the formation and lifetime of Ps in biomaterials, it is important to have knowledge about the interaction of positrons with organic molecules. In this aspect, the interactions between positrons and benzene are interesting. The available data for positron–benzene scattering include the measured total cross-sections (TCSs) by Sueoka [17], Makochekanwa [18], Karwasz et al. [19,20], and Zecca et al. [21]. The elastic cross-section for low collision energies has been computed by Kimura et al. [22], Occhigrossi and Gianturco [23], Franz and Franz [24], Karbowski et al. [25], and Barbosa et al. [26]. Barbosa et al. [26] also present cross-sections for direct ionization, excitation, and Ps formation. Lino [27] has computed the cross-section for electronic excitation. The datasets for electronic excitation cross-sections are very different from each other. In this paper, we present new calculations of the cross-sections for direct ionization using binary-encounter Bethe models [28,29] and for electronic excitation using the binary-encounter Born approximation [30]. Furthermore, we present an estimation of the cross-section for Ps formation by subtracting the elastic cross-section and the cross-sections for direction ionization and electronic excitation from the experimental total cross-section.

This paper is organized in the following way. Theoretical models and computational procedures of the calculations are summarized in Section 2. The results are presented and discussed in Section 3. The paper ends with our conclusions in Section 4.

2. Theory and Computational Details

2.1. Molecular Structure

The conducted simulations concern collisions between a positron and the benzene molecule. Benzene is a cyclic organic molecule containing six carbon atoms and six hydrogen atoms, displaying a hexagonal, planar structure. The program package Gaussian

v16 was employed to optimize the structure of the benzene molecule using the Density Functional Theory (DFT) [31]. The Becke, 3-parameter, Lee–Yang–Parr (B3LYP) exchange-correlation functional [32,33] and the 6-311++G(2df,2p) basis set [34] are used. The optimized parameters are 1.391 Angstrom for the CC bond length and 1.082 Angstrom for the CH bond length.

2.2. Model for Direct Ionization of Molecules by Positron Impact

The binary-encounter Bethe (BEB) model [35,36] is one of the most frequently used and successful models for the calculation of cross-sections for ionization by electron impact. Fedus and Karwasz [28] derived binary-encounter Bethe models for positrons BEB-0 and BEB-W. The BEB-W model takes into account the Wannier threshold law [37]. Franz et al. [29] present the models BEB-A and BEB-B, which follow the threshold law of Jansen et al. [38]. These models allow accurate results to be obtained over a large range of energies and give ionization cross-sections which are close to experimental data [14,39] and ab initio calculations [40].

Here we give a short summary of the BEB-0, BEB-W, BEB-A and BEB-B models. More details can be found in the original publications [28,29]. The total cross-section (σ_{ion}) for the direct ionization of a molecule by positron impact can be written as the sum of the partial ionization cross-section (σ_i^{ion}) for ionization out of the occupied molecular orbitals.

$$\sigma_{\mathrm{ion}}(E) = \sum_{i}^{n_{\mathrm{occ}}} \sigma_i^{\mathrm{ion}}(E) \; . \tag{1}$$

Here, the sum runs over all n_{occ} occupied orbitals. In the following, E is the kinetic energy of the incoming positron, B_i is the binding energy of the electron in molecular orbital i, and U_i is the expectation value of the kinetic energy of the electron in orbital i. The formulas can be expressed in reduced quantities:

$$t_i = \frac{E}{B_i} \;\; and \;\; u_i = \frac{U_i}{B_i} \; . \tag{2}$$

The general formula for the partial ionization cross-section is given by

$$\sigma_i^{\mathrm{ion}} = \frac{S_i}{t_i + u_i + 1 + f_i} \left[\frac{\ln(t_i)}{2} (1 - \frac{1}{t_i^2}) + h_i (1 - \frac{1}{t_i}) + G_i \right] \; , \tag{3}$$

where the prefactor is given by

$$S_i = 4\pi a_0^2 N_i (\frac{R}{B_i})^2 \; , \tag{4}$$

where $a_0 = 0.529 \times 10^{-10}$ m is the Bohr radius, $R = 13.6$ eV is the Rydberg constant, and N_i is the number of electrons in orbital number i. The various models can be defined as follows:

- BEB-0 model: $f_i = 0$, $h_i = 1$, $G_i = 0$.
- BEB-W model: $f_i = f_i^{\mathrm{W}}$, $h_i = 1$, $G_i = 0$ with the term

$$f_i^{\mathrm{W}} = \frac{1}{(t_i - 1)^{1.65}} \; . \tag{5}$$

- BEB-A model: $f_i = f_i^{\mathrm{A}}$, $h_i = 1$, $G_i = 0$ with the term

$$f_i^{\mathrm{A}} = \frac{1}{(t_i - 1)^{\alpha - 1} e^{-\beta_i \sqrt{t_i - 1}}}\,, \tag{6}$$

  where $\alpha = 2.64$ and $\beta_i = 0.489\sqrt{\frac{B_i}{2R}}$ to fulfill the threshold law of Jansen et al. [38].
- BEB-B model: $f_i = 0$, $h_i = 1 - g_i(t_i)$, $G_i = g_i(t_i)\left(1 - \frac{1}{t_i}\right)^{\alpha}$ and $g_i(t_i) = e^{\beta_i \sqrt{t_i - 1}}$ with the same values for α and β_i as in the BEB-A model.

For the calculation of the ionization cross-section, the binding energies and the expectation values of the kinetic energy of the electron before its removal are presented in Table 1. The binding energies for the lowest orbitals are calculated using Koopmans' theorem [41]. For the outer valence orbitals, Koopmans' theorem is not accurate enough, and therefore, we employ the Outer Valence Green Function (OVGF) method [42] for the highest seven orbitals.. The program package Gaussian v16 [31] is used for all calculations with the 6-311++G(2df,2p) basis set [34]. In our computation, we obtain 9.26 eV for the lowest ionization energy, which is close to the experimental value of 9.24 eV for the vertical ionization energy obtained by Karlsson et al. [43].

Table 1. Computed binding energies B_i, expectation values of the kinetic energies U_i, and occupation numbers N_i of the molecular orbitals of benzene.

Orbital	B_i/eV	U_i/eV	N_i
$1e_{1g}$	9.26 [a]	27.81	4
$3e_{2g}$	12.16 [a]	37.81	4
$1a_{2u}$	12.45 [a]	23.70	2
$3e_{1u}$	14.47 [a]	32.46	4
$1b_{2u}$	14.90 [a]	39.91	2
$2b_{1u}$	15.82 [a]	34.21	2
$3a_{1g}$	17.40 [a]	25.33	2
$2e_{2g}$	22.44 [b]	39.03	4
$2e_{1u}$	27.64 [b]	42.36	4
$2a_{1g}$	31.36 [b]	39.36	2
$1b_{1u}$	305.62 [b]	436.29	2
$1e_{1u}$	305.64 [b]	436.11	4
$1e_{2g}$	305.68 [b]	435.74	4
$1a_{1g}$	305.69 [b]	435.59	2

[a] Binding energy calculated with the OVGF method. [b] Binding energy calculated using Koopmans' theorem.

Cross-Sections for Electronic Excitation

The total cross-section for electronic excitation is given by the sum of cross-sections for electronic excitation from the electronic ground state to excited states Y.

$$\sigma_{\mathrm{elec}} = \sum_Y \sigma_{0Y}^{\mathrm{elec}}. \tag{7}$$

The cross-section for each electronically excited state is calculated using the binary-encounter-scaled Born cross-section [30]

$$\sigma_{0Y}^{\mathrm{elec}} = \frac{E}{E + B_i + \Delta E_{0Y}} \sigma_{0Y}^{\mathrm{Born}}\,. \tag{8}$$

Here, ΔE_{0Y} is the excitation energy from the electronic ground state to the excited state Y and $\sigma_{0Y}^{\text{Born}}$ is the cross-section for electronic excitation within the first Born approximation [44].

$$\sigma_{0Y}^{\text{Born}} = \frac{8\pi}{3k_0^2} D_{0Y}^2 \ln\left|\frac{k_0 + k_Y}{k_0 - k_Y}\right|. \tag{9}$$

Here, D_{0Y} is the transition dipole moment between the electronic ground state and the electronically excited state Y of the molecule. The wavenumbers of the electron before (k_0) and after (k_Y) collision are given by

$$k_0 = \frac{1}{\hbar}\sqrt{2m_e E} \quad \text{and} \quad k_Y = \frac{1}{\hbar}\sqrt{2m_e(E - \Delta E_{0Y})}\,, \tag{10}$$

For the calculation of the electronically inelastic cross-section, we used the energies and oscillator strength from Li et al. [45], obtained with the symmetry-adapted cluster–configuration interaction (SAC-CI) method. In Table 2, we show the data for all dipole-allowed transitions obtained by Li et al. [45]. All three electronic excitations are transitions of one electron from the highest occupied molecular orbital (here denoted as π) to a virtual orbital. The transition dipole moment and the oscillator strength are connected through the equation

$$f_{0Y} = \frac{2}{3}\frac{m_e \Delta E_{0Y}}{\hbar^2}|D_{0Y}|^2\,. \tag{11}$$

For the binary-encounter scaling, we used the binding energy $B_i = 9.26$ eV for the $1e_{1g}$ orbital from Table 1.

Table 2. Electronically excited states of benzene with non-zero oscillator strength. All states have been computed using SAC-CI by Li et al. [45].

Excited State Y	Description	f_{0Y}	ΔE/eV
1^1E_{1u}	Rydberg $\pi \rightarrow \pi^*$	0.2021	7.06
2^1E_{1u}	Valence $\pi \rightarrow \pi^*$	0.6204	7.48
1^1A_{2u}	Rydberg $\pi \rightarrow \sigma^*$	0.0350	7.06

3. Results and Discussion

In Figure 1, we present the cross-sections for the direct ionization of the benzene molecule by positron impact and compare them with available results from the literature. The figure shows the computed ionization cross-section, which is obtained with the four BEB models and the calculations by Barbosa et al. [26] using the independent atom model with the screening-corrected additivity rule including interference effects (IAM-SCAR+I) method. From Figure 1, it can be seen that for collision energies below 40 eV, the IAM-SCAR+I method gives the largest cross-section. The results, obtained with the four BEB models, are relatively close together, where BEB-0 gives the largest cross-sections, followed by BEB-W, BEB-B, and BEB-A. The IAM-SCAR+I reaches a maximum at 40 eV. In contrast, BEB-0 has its maximum at 59 eV, BEB-W at 63 eV, BEB-A at 71 eV, and BEB-B at 72 eV. For collision energies above 200 eV, all four BEB curves converge, and the lines are not distinguishable in Figure 1 and are slightly above the IAM-SCAR+I curve. In our previous study of positron impact ionization, we obtained the best results for neutral molecules with the BEB-A and BEB-B models. Therefore, we will use the BEB-B results in our calculation of the TCS.

In Figure 2, we show the cross-sections for the direct ionization for each valence orbital. For the computations, we used the BEB-B model. We can see that the largest contribution is due to the highest molecular orbital. In Figure 3, we show the contributions of the four core orbitals. The cross-sections for each of the four core orbitals are below 0.01×10^{-20} m^2.

The parameters B_i and U_i are the same for all four orbitals. Due to the degeneracy of the orbitals $1e_{1u}$ and $1e_{2g}$, their cross-sections are two times larger than the cross-sections for the ionization from the orbitals $1b_{1u}$ and $1a_{1g}$.

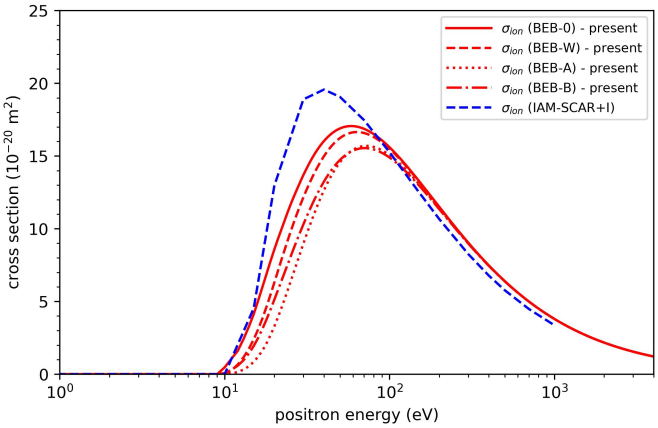

Figure 1. Direct ionization cross-section from benzene molecules by positron impact. The results from calculations with the four different BEB models are shown by a solid red line (BEB-0), dashed red line (BEB-W), dotted red line (BEB-A), and dash–dotted red line (BEB-B). The data from calculations by Barbosa et al. [26] with the IAM-SCAR+I method are shown by the dashed blue line.

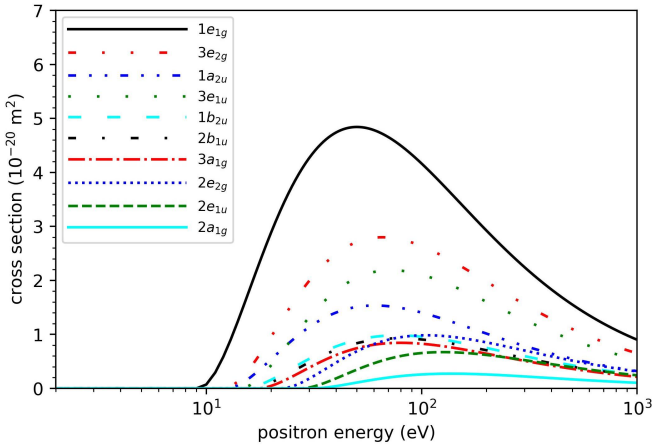

Figure 2. Direct ionization cross-section from benzene molecules by positron impact for the valence orbitals computed with the BEB-B model.

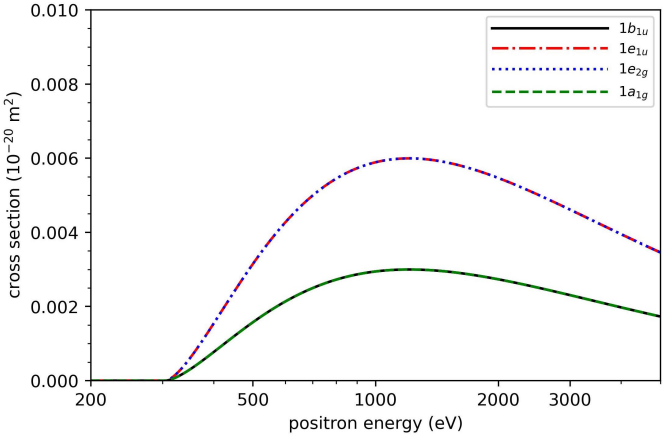

Figure 3. Direct ionization cross-section from benzene molecules by positron impact for the core orbitals computed with the BEB-B model. The cross-sections for the orbitals $1e_{1u}$ and $1e_{2g}$ cannot be distinguished from each other. The same applies for the orbitals $1b_{1u}$ and $1a_{1g}$.

Regarding the electronic excitations of benzene by positron impact, calculations have been performed by Barbosa et al. [26] using the IAM-SCAR+I method and by Lino [27] using the scaling Born positron (SBP) approach. Figure 4 shows our results using the BE-scaled Born approximation together with the results of the IAM-SCAR+I method [26] and the SBP approach [27]. The curve with BE-scaled cross-sections reaches a maximum of 6.92×10^{-20} m^2 at 15 eV. The IAM-SCAR+I results show a maximum value of 15.26×10^{-20} m^2 at the same energy and are larger than our results for nearly all collision energies, with the exception of a small energy range between 30 and 60 eV. The SBP results reach their maximum value of 2.98×10^{-20} m^2 at 30 eV. This is much smaller than our results and the IAM-SCAR+I results.

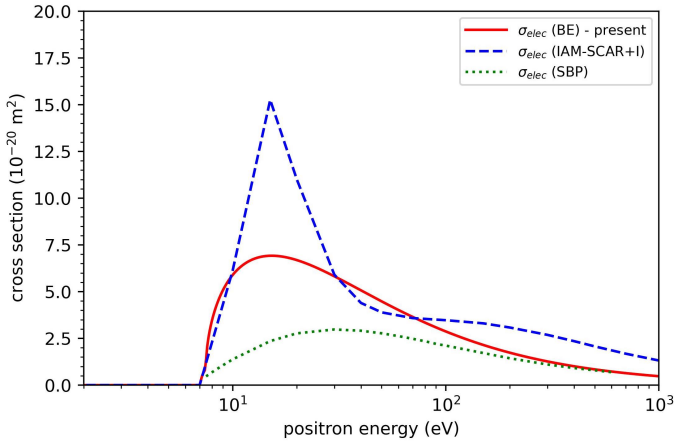

Figure 4. Integral cross-sections for positron impact excitation of electronic states in benzene. Present calculations using the BE-scaled Born approximation are shown by the solid red line. Also shown are IAM-SCAR+I results [26] (dashed blue line) and SBP results [27] (green dotted line).

It is also important to note that our calculations are for excitation into the excited states 1^1E_{1u}, 2^1E_{1u} and 1^1A_{2u}. The cross-sections for the excitation of each state are shown in Figure 5. All three states are dipole allowed (the transition dipole moment between the ground state and the excited state is non-zero). Lino studied transitions into $^1E_{1u}$ and the dipole-forbidden state $^1B_{1u}$. Barbosa et al. [26] do not specify the electronic states that they consider in their calculation.

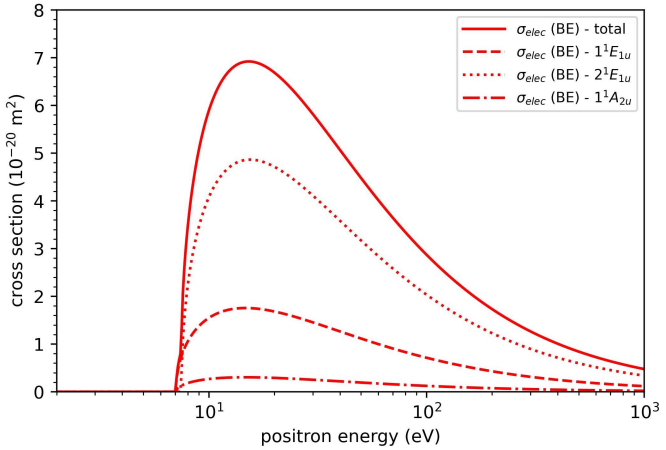

Figure 5. Integral cross-sections for positron impact excitation of electronic states in benzene. Present calculations using the BE-scaled Born approximation.

In Figure 6, we show our estimate of the total cross-section, excluding the cross-section for Ps formation.

$$\sigma_{total-Ps} = \sigma_{el} + \sigma_{ion} + \sigma_{elec}. \quad (12)$$

Here, we sum the elastic cross-section σ_{el}, the cross-section for direct ionization σ_{ion} and the cross-section for electronic excitation σ_{elec}. The elastic cross-section is taken from Franz and Franz [29], which is obtained by the R-matrix method with enhancement factors. The ionization cross-section is computed with the BEB-B method and the cross-section for electronic excitation uses the BE-scaled Born approximation. In Figure 6, we present the total cross-sections obtained by the IAM-SCAR+I method [26] and experimental results by Sueoka [17], Makochekanwa et al. [18], Zecca et al. [21], and Karwasz et al. [19,20]. Barbosa et al. [26] calculated corrections for the angular discrimination error in the experiment by Zecca et al. [21] for collision energies below 1 eV. These corrections bring Zecca's results very close to Sueoka's results, but are not shown in Figure 6. It should be noted that the results of Makochekanwa et al. [18] are considered too low at collision energies below 50 eV. A detailed discussion about these results can be found in the review by Brunger et al. [14]. For energies below 2 eV, the IAM-SCAR+I cross-sections are lower than the experimental cross-sections, whereas for energies larger than 2 eV, they are the largest cross-sections in the figure. The IAM-SCAR+I cross-sections show a maximum around 10 eV, which is absent in all other datasets.

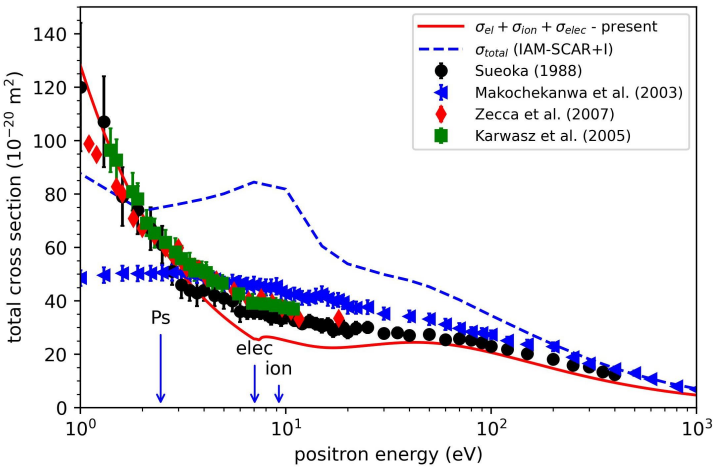

Figure 6. Total cross-sections for positron collisions with benzene. Present results are shown by the solid red line. Also shown are results obtained with the IAM-SCAR+I method (dashed blue line) and experimental results by Sueoka [17] (black circles), Makochekanwa et al. [18] (blue triangles), Zecca et al. [21] (red diamonds), and Karwasz et al. [19,20] (green squares). The thresholds for Ps formation, electronic excitation, and direct ionization are marked with arrows.

Brunger et al. [14] recommend the experimental values from Zecca et al. [21] as the total cross-section for low energies and the values from Sueoka [17] for large collision energies. For energies below the threshold for Ps formation and for energies above 30 eV, the sum of our cross-section $\sigma_{total-Ps}$ is very close to the experimental data points from Karwasz et al. [19,20] and Sueoka [17]. In the range between 3 and 30 eV, the sum of our cross-sections is smaller than the recommended cross-section. We assume that this difference is due to Ps formation. For an estimation of the cross-section for Ps formation,

$$\sigma_{Ps} = \sigma_{total}^{\text{recommended}} - \sigma_{total-Ps}$$

we subtract the sum $\sigma_{total-Ps}$ of our cross-sections from the recommended total cross-section $\sigma_{total}^{\text{recommended}}$ from Brunger et al. [14]. The estimated cross-section for Ps formation

is shown in Figure 7 together with the cross-section for Ps formation from Barbosa et al. [26] obtained with the IAM-SCAR+I method. Also shown is one experimental data point at an energy 2 eV above the threshold from measurements by Sueoka et al. [46]. The maximum of our estimated cross-section is about 15×10^{-20} m^2, which is of a similar magnitude to the maximum of the IAM-SCAR+I cross-section. Our estimated cross-section shows several oscillations, which are due to the oscillations in the recommended experimental cross-sections. These are clearly not physical features like resonances. For large collision energies, our estimated cross-section reaches a value of roughly 3×10^{-20} m^2. This might be an indication that our elastic cross-section is too small for larger collision energies.

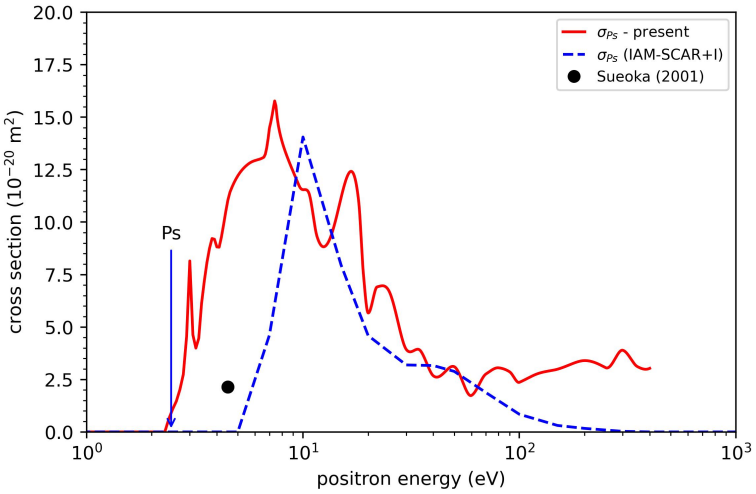

Figure 7. Cross-sections for Ps formation in positron collisions with benzene. Present results are shown by the solid red line. Also shown are results obtained with the IAM-SCAR+I method (dashed blue line) and experimental results by Sueoka [17] (black circle). The threshold for Ps formation is marked with an arrow.

4. Conclusions

In this manuscript, we present cross-sections for direct ionization and electronic excitation in collisions of positrons with benzene molecules. Four theoretical models based on binary-encounter Bethe theory are used to calculate ionization cross-sections. Our results are slightly lower than those from Barbosa et al. [26] obtained with the IAM-SCAR+I method for energies below 100 eV. For the calculation of cross-sections for electronic excitation, we employed the binary-encounter Born approximation. Our results are between those obtained by Barbosa et al. with the IAM-SCAR+I method and those by Lino [27] with the SBP approach. Finally, we obtain an estimate of the cross-section for Ps formation by subtraction of the elastic cross-section and the cross-sections for direct ionization and electronic excitation from the recommended experimental total cross-section. The obtained Ps cross-section has a peak of the same magnitude as results obtained with the IAM-SCAR+I method.

Author Contributions: Conceptualization, M.F. and J.F.; methodology, M.F. and J.F.; software, A.P., M.F. and J.F.; validation, A.P., M.F. and J.F.; formal analysis, M.F. and J.F.; investigation, A.P., M.F. and J.F.; resources, J.F.; data curation, M.F. and J.F.; writing—original draft preparation, M.F. and J.F.; writing—review and editing, M.F. and J.F.; visualization, M.F. and J.F.; supervision, M.F. and J.F.; project administration, M.F.; funding acquisition, J.F. All authors have read and agreed to the published version of the manuscript.

Funding: The research has been supported by the computer center WCSS (Wroclawskie Centrum Sieciowo-Superkomputerowe, Politechnika Wroclawska) through grant number KDM-408.

Institutional Review Board Statement: Not applicable.

Informed Consent Statement: Not applicable.

Data Availability Statement: The data that support the findings of this study will be soon openly available in the MOST Wiedzy repository (https://mostwiedzy.pl/en/open-research-data/catalog) (accessed on 25 December 2024).

Acknowledgments: The authors thank Alessandra Souza Barbosa and M. H. F. Bettega for sending us the data from Barbosa et al. [26].

Conflicts of Interest: The authors declare no conflicts of interest.

Abbreviations

The following abbreviations are used in this manuscript:

BE	binary-encounter
BEB	binary-encounter Bethe
BEB-0	binary-encounter Bethe for positrons
BEB-W	binary-encounter Bethe for positrons with Wannier-type threshold law
BEB-A	binary-encounter Bethe for positrons with Jansen-type threshold law, version A
BEB-B	binary-encounter Bethe for positrons with Jansen-type threshold law, version B
B3LYP	Becke, 3-parameter, Lee–Yang–Parr exchange-correlation functional
DFT	Density Functional Theory
eV	electron volt
IAM-SCAR+I	independent atom model with the screening corrected additivity rule, including interference
ISM	interstellar medium
OVGF	Outer Valence Green Function
PAH	polycyclic aromatic hydrocarbon
PET	positron emission tomography
Ps	positronium
SAC-CI	symmetry adapted cluster-configuration interaction
SBP	scaling Born positron

References

1. Bass, S.D.; Mariazzi, S.; Moskal, P.; Stepien, E. Positronium Physics and Biomedical Applications. *Rev. Mod. Phys.* **2023**, *95*, 021002. [CrossRef]
2. Dryzek, J. *Positron Profilometry Probing Material Depths for Enhanced Understanding*, 1st ed.; Springer: Cham, Switzerland, 2023.
3. Keeble, D.J.; Wiktor, J.; Pathak, S.K.; Phillips, L.J.; Dickmann, M.; Durose, K.; Snaith, H.J.; Egger, W. Identification of lead vacancy defects in lead halide perovskites. *Nat. Com.* **2021**, *12*, 5566. [CrossRef] [PubMed]
4. Prantzos, N.; Boehm, C.; Bykov, A.M.; Diehl, R.; Ferriére, K.; Guessoum, N.; Jean, P.; Knoedlseder, J.; Marcowith, A.; Moskalenko, I.V.; et al. The 511 keV emission from positron annihilation in the Galaxy. *Rev. Mod. Phys.* **2011**, *83*, 1001. [CrossRef]
5. Casse, M.; Paul, J.; Bertone, G.; Sigl, G. Gamma Rays from the Galactic Bulge and Large Extra Dimensions. *Phys. Rev. Lett.* **2004**, *92*, 111102. [CrossRef] [PubMed]
6. Boehm, C.; Hooper, D.; Silk, J.; Casse, M.; Paul, J. MeV Dark Matter: Has It Been Detected? *Phys. Rev. Lett.* **2004**, *92*, 101301. [CrossRef] [PubMed]
7. Paul, J. Positrons in the universe. *Nucl. Instrum. Methods Phys. Res. B* **2004**, *221*, 215–224. [CrossRef]
8. Aguilar, M.; Ali Cavasonza, L.; Ambrosi, G.; Arruda, L.; Attig, N.; Azzarello, P.; Bachlechner, A.; Barao, F.; Barrau, A.; Barrin, L.; et al. Towards Understanding the Origin of Cosmic-Ray Positrons. *Phys. Rev. Lett.* **2019**, *122*, 041102. [CrossRef] [PubMed]
9. Guessoum, N.; Jean, P.; Prantzos, N. Microquasars as sources of positron annihilation radiation. *Astron. Astrophys.* **2006**, *457*, 753–762. [CrossRef]
10. Guessoum, N.; Jean, P.; Gillard, W. Positron annihilation on polycyclic aromatic hydrocarbon molecules in the interstellar medium. *Mon. Not. R. Astron. Soc.* **2010**, *402*, 1171–1178. [CrossRef]
11. Surko, C.M.; Gribakin, G.F.; Buckman, S.J. Low-energy positron interactions with atoms and molecules. *J. Phys. B At. Mol. Phys.* **2005**, *38*, R57. [CrossRef]

12. Dapor, M. *Transport of Energetic Electrons in Solids*, 3rd ed.; Springer: Cham, Switzerland, 2023.
13. Franz, M.; Franz, J. A Monte Carlo strategy to simulate positrons and positronium in biological materials. *Bio-Algorithms Med-Syst.* **2023**, *19*, 40–42. [CrossRef]
14. Brunger, M.J.; Buckman, S.J.; Ratnavelu, K. Positron Scattering from Molecules: An Experimental Cross Section Compilation for Positron Transport Studies and Benchmarking Theory. *J. Phys. Chem. Ref. Data* **2017**, *46*, 023102. [CrossRef]
15. Moskal, P.; Stepien, E. Positronium as a biomarker of hypoxia. *Bio-Algorithms Med-Syst.* **2021**, *17*, 311–319. [CrossRef]
16. Steinberger, W.M.; Mercolli, L.; Breuer, J.; Sari, H.; Parzych, S.; Niedzwiecki, S.; Lapkiewicz, G.; Moskal, P.; Stepien, E.; Rominger, A.; et al. Developing a Novel Positronium Biomarker for Cardiac Myxoma Imaging. *EJNMMI Phys.* **2023**, *10*, 76.
17. Sueoka, O. Total cross section measurements for positron and electron scattering on benzene molecules. *J. Phys. B At. Mol. Opt. Phys.* **1988**, *21*, L631. [CrossRef]
18. Makochekanwa, C.; Sueoka, O.; Kimura, M. Comparative study of electron and positron scattering from benzene (C6H6) and hexafluorobenzene (C6F6) molecules. *Phys. Rev. A* **2003**, *68*, 032707. [CrossRef]
19. Karwasz, G.P.; Pliszka, D.; Zecca, A.; Brusa, R.S. Total cross sections for positron scattering on benzene and nitrogen. *J. Phys. B At. Mol. Opt. Phys.* **2005**, *38*, 1–13.
20. Karwasz, G.P.; Karbowski, A.; Idziaszek, Z.; Brusa, R.S. Total cross sections for positron scattering on benzene - angular resolution corrections. *Nucl. Instrum. Methods Phys. Res. B* **2008**, *266*, 471–477. [CrossRef]
21. Zecca, A.; Moser, N.; Perazzolli, C.; Salemi, A.; Brunger, M.J. Total cross sections for positron scattering from benzene, cyclohexane, and aniline. *Phys. Rev. A* **2007**, *76*, 022708. [CrossRef]
22. Kimura, M.; Makochekanwa, C.; Sueoka, O. Contrasting low-energy behaviour in total cross sections for electron and positron scattering from benzene molecules. *J. Phys. B At. Mol. Opt. Phys.* **2004**, *37*, 1461. [CrossRef]
23. Occhigrossi, A.; Gianturco, F.A. Low-energy positron dynamics in small hydrocarbon gases. *J. Phys. B At. Mol. Opt. Phys.* **2003**, *36*, 1383. [CrossRef]
24. Franz, J.; Franz, M. Low-energy positron scattering from gas-phase benzene. *Eur. Phys. J. D* **2019**, *73*, 192. [CrossRef]
25. Karbowski, A.; Karwasz, G.P.; Franz, M.; Franz, J. Positron Scattering and Annihilation in Organic Molecules. *Acta Phys. Pol. B* **2020**, *51*, 207–212. [CrossRef]
26. Barbosa, A.S.; Blanco, F.; Garcia, G.; Bettega, M.H.F. Theoretical study on positron scattering by benzene over a broad energy range. *Phys. Rev. A* **2019**, *100*, 062705. [CrossRef]
27. Lino, J.L.S. Electronic excitation of C_6H_6 by positron impact. *Rev. Mex. Fis.* **2021**, *67*, 188–192. [CrossRef]
28. Fedus, K.; Karwasz, G. Binary-encounter dipole model for positron-impact direct ionization. *Phys. Rev. A* **2019**, *100*, 062702. [CrossRef]
29. Franz, M.; Wiciak-Pawlowska, K.; Franz, J. Binary-encounter model for direct ionization of molecules by positron-impact. *Atoms* **2021**, *9*, 99. [CrossRef]
30. Kim, Y.-K. Scaled Born cross sections for excitations of H_2 by electron impact. *J. Chem. Phys.* **2007**, *126*, 064305. [CrossRef]
31. Frisch, M.J.; Trucks, G.W.; Schlegel, H.B.; Scuseria, G.E.; Robb, M.A.; Cheeseman, J.R.; Scalmani, G.; Barone, V.; Petersson, G.A.; Nakatsuji, H.; et al. *Gaussian 16, Revision C.01*; Gaussian Inc.: Wallingford, CT, USA, 2016.
32. Becke, A.D. Density-functional thermochemistry. III. The role of exact exchange. *J. Chem. Phys.* **1993**, *98*, 5648–5652. [CrossRef]
33. Lee, C.; Yang, W.; Parr, R.G. Development of the Colle-Salvetti correlation-energy formula into a functional of the electron density. *Phys. Rev. B* **1988**, *37*, 785–789. [CrossRef] [PubMed]
34. Raghavachari, K.; Binkley, J.S.; Seeger, R.; Pople, J.A. Self-Consistent Molecular Orbital Methods. 20. Basis set for correlated wave-functions. *J. Chem. Phys.* **1980**, *72*, 650–654.
35. Kim, Y.-K.; Rudd, M.E. Binary-encounter-dipole model for electron-impact ionization. *Phys. Rev. A* **1994**, *50*, 3954–3967. [CrossRef]
36. Hwang, W.; Kim, Y.-K.; Rudd, M.E. New model for electron-impact ionization cross sections of molecules. *J. Phys. Chem.* **1995**, *104*, 2956–2966. [CrossRef]
37. Wannier, G.H. The Threshold Law for Single Ionization of Atoms or Ions by Electrons. *Phys. Rev.* **1953**, *90*, 817–825. [CrossRef]
38. Jansen, K.; Ward, S.J.; Shertzer, J.; Macek, J.H. Absolute cross sections for positron impact ionization of hydrogen near threshold. *Phys. Rev. A* **2009**, *79*, 022704. [CrossRef]
39. Ratnavelu, K.; Brunger, M.J.; Buckman, S.J. Recommended positron scattering cross sections for atomic systems. *J. Phys. Chem. Ref. Data* **2019**, *48*, 023102. [CrossRef]
40. Utamuratov, R.; Kadyrov, A.S.; Fursa, D.V.; Zammit, M.C.; Bray, I. Two-center close-coupling calculations for positron-molecular-hydrogen scattering. *Phys. Rev. A* **2015**, *92*, 032707. [CrossRef]
41. Koopmans, T. Ordering of Wave Functions and Eigenenergies to the Individual Electrons of an Atom. *Physica* **1933**, *1*, 104–113. [CrossRef]
42. von Niessen, W.; Schirmer, J.; Cederbaum, L.S. Computational methods for the one-particle Green's function. *Comp. Phys. Rep.* **1984**, *1*, 57–125. [CrossRef]

43. Karlsson, L.; Mattsson, L.; Jadrny, R.; Bergmark, T.; Siegbahn, K. Valence Electron Spectra of Benzene and the Hexafluorides of Sulphur, Molybdenum, Tungsten and Uranium. *Phys. Scr.* **1976**, *14*, 230–241. [CrossRef]
44. Lane, N.F. The theory of electron—Molecule collisions. *Rev. Mod. Phys.* **1980**, *52*, 29–119. [CrossRef]
45. Li, Y.; Wan, J.; Xu, X. Theoretical study of the vertical excited states of benzene, pyrimidine, and pyrazine by the symmetry adapted cluster configuration interaction method. *J. Comput. Chem.* **2007**, *28*, 1658–1667. [CrossRef] [PubMed]
46. Sueoka, O.; Kawada, M.K.; Kimura, M. Total and positronium formation cross-sections in polyatomic molecules. *Nucl. Instrum. Methods Phys. Res. B* **2000**, *171*, 96–102. [CrossRef]